COLEÇÃO

DESAFIOS DAS ENGENHARIAS:

ENGENHARIA ELÉTRICA 2

JOÃO DALLAMUTA
HENRIQUE AJUZ HOLZMANN
(ORGANIZADORES)

Atena Editora
Ano 2021

COLEÇÃO

DESAFIOS DAS ENGENHARIAS:

ENGENHARIA ELÉTRICA 2

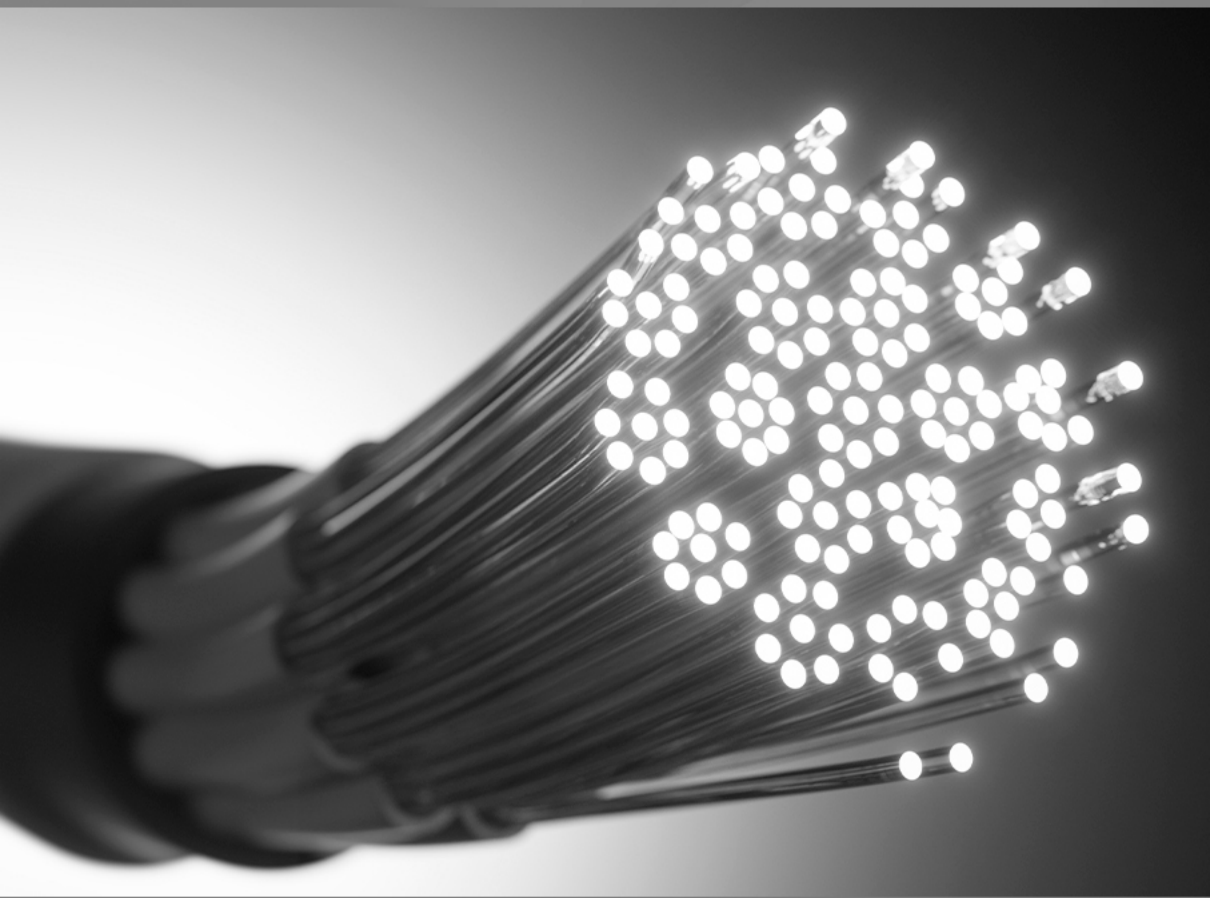

JOÃO DALLAMUTA
HENRIQUE AJUZ HOLZMANN
(ORGANIZADORES)

Atena
Editora
Ano 2021

Editora chefe
Profª Drª Antonella Carvalho de Oliveira
Editora executiva
Natalia Oliveira
Assistente editorial
Flávia Roberta Barão
Bibliotecária
Janaina Ramos
Projeto gráfico
Camila Alves de Cremo
Daphynny Pamplona
Luiza Alves Batista
Maria Alice Pinheiro
Natália Sandrini de Azevedo
Imagens da capa
iStock
Edição de arte
Luiza Alves Batista

Atena
Editora
Ano 2021

Ciências Exatas e da Terra e Engenharias

Atena Editora
Ano 2021

Ciências Exatas e da Terra e Engenharias

Coleção desafios das engenharias: engenharia elétrica 2

Diagramação: Daphynny Pamplona
Correção: Flávia Roberta Barão
Indexação: Gabriel Motomu Teshima
Revisão: Os autores
Organizadores: João Dallamuta
Henrique Ajuz Holzmann

Dados Internacionais de Catalogação na Publicação (CIP)

C691 Coleção desafios das engenharias: engenharia elétrica 2 / Organizadores João Dallamuta, Henrique Ajuz Holzmann. – Ponta Grossa - PR: Atena, 2021.

Formato: PDF
Requisitos de sistema: Adobe Acrobat Reader
Modo de acesso: World Wide Web
Inclui bibliografia
ISBN 978-65-5983-556-0
DOI: https://doi.org/10.22533/at.ed.560211910

1. Engenharia elétrica. I. Dallamuta, João (Organizador). II. Holzmann, Henrique Ajuz (Organizador). III. Título.

CDD 621.3

Elaborado por Bibliotecária Janaina Ramos – CRB-8/9166

Atena Editora
Ponta Grossa – Paraná – Brasil
Telefone: +55 (42) 3323-5493
www.atenaeditora.com.br
contato@atenaeditora.com.br

Ano 2021

DECLARAÇÃO DOS AUTORES

Os autores desta obra: 1. Atestam não possuir qualquer interesse comercial que constitua um conflito de interesses em relação ao artigo científico publicado; 2. Declaram que participaram ativamente da construção dos respectivos manuscritos, preferencialmente na: a) Concepção do estudo, e/ou aquisição de dados, e/ou análise e interpretação de dados; b) Elaboração do artigo ou revisão com vistas a tornar o material intelectualmente relevante; c) Aprovação final do manuscrito para submissão.; 3. Certificam que os artigos científicos publicados estão completamente isentos de dados e/ou resultados fraudulentos; 4. Confirmam a citação e a referência correta de todos os dados e de interpretações de dados de outras pesquisas; 5. Reconhecem terem informado todas as fontes de financiamento recebidas para a consecução da pesquisa; 6. Autorizam a edição da obra, que incluem os registros de ficha catalográfica, ISBN, DOI e demais indexadores, projeto visual e criação de capa, diagramação de miolo, assim como lançamento e divulgação da mesma conforme critérios da Atena Editora.

Ciências Exatas e da Terra e Engenharias

Atena Editora
Ano 2021

DECLARAÇÃO DA EDITORA

Atena Editora
Ano 2021

APRESENTAÇÃO

A engenharia elétrica tornou-se uma profissão há cerca de 130 anos, com o início da distribuição de eletricidade em caráter comercial e com a difusão acelerada do telégrafo em escala global no final do século XIX.

Na primeira metade do século XX a difusão da telefonia e da radiodifusão além do crescimento vigoroso dos sistemas elétricos de produção, transmissão e distribuição de eletricidade, deu os contornos definitivos para a carreira de engenheiro eletricista que na segunda metade do século, com a difusão dos semicondutores e da computação gerou variações de ênfase de formação como engenheiros eletrônicos, de telecomunicações, de controle e automação ou de computação.

Produzir conhecimento em engenharia elétrica é portando pesquisar em uma gama enorme de áreas, subáreas e abordagens de uma engenharia que é onipresente em praticamente todos os campos da ciência e tecnologia.

Neste livro temos uma diversidade de temas, níveis de profundidade e abordagens de pesquisa, envolvendo aspectos técnicos e científicos. Aos autores e editores, agradecemos pela confiança e espirito de parceria.

João Dallamuta

Henrique Ajuz Holzmann

SUMÁRIO

CAPÍTULO 1 1

PHOTODETECTOR OPTIC POWER OPTIMIZATION TO INCREASE THE GAIN ON SUB-OCTAVE MICROWAVE PHOTONIC LINK

Naiara Tieme Mippo
Paulo Henrique Kiohara Acyoli Bastos
Felipe Streitenberger Ivo
Olympio Lucchini Coutinho

https://doi.org/10.22533/at.ed.5602119101

CAPÍTULO 2 14

OPTOELECTRONIC SENSOR APPLIED TO FLOW RATE MEASUREMENTS ON OIL AND GAS INDUSTRY

Alexandre Silva Allil
Fabio da Silva Dutra
Cesar Cosenza de Carvalho
Regina Célia da Silva Barros Allil
Marcelo Martins Werneck

https://doi.org/10.22533/at.ed.5602119102

CAPÍTULO 3 25

ANÁLISE DO ENVELHECIMENTO, PRECISÃO E EXATIDÃO EM SENSORES ÓTICOS FBG E RFBG QUE MEDEM TEMPERATURAS ENTRE 5 °C E 60 °C POR 16 SEMANAS

Karoline Akemi Sato
Camila Carvalho de Moura
Antonio Carlos Ribeiro Filho
Luis Camilo Jussiani Moreira
Valmir de Oliveira

https://doi.org/10.22533/at.ed.5602119103

CAPÍTULO 4 38

EVALUACIÓN PARA INVERSIÓN CON OPTIMIZACIÓN DE SECCIÓN CONDUCTOR Y TENSIÓN DE DISTRIBUCIÓN. APLICACIÓN DE LOS ALGORITMOS DEL LEY DE KELVIN

Christian Arturo Ramirez Osorio
Enrique Buzarquis
Rodney Damián Fariña Martínez

https://doi.org/10.22533/at.ed.5602119104

CAPÍTULO 5 55

STRATEGIES OF VOLTAGE CONTROL BASED IN FUZZY LOGIC ALGORITHMS WITH ALTERNATIVE, CLEAN AND RENEWABLE GENERATION OPERATING WITH ANOTHER CONVENTIONAL ELECTRIC GENERATION IN WITH RADIAL LOADS IN POWER SYSTEMS STABILITY

Rodney Damián Fariña Martínez
Antonio Carlos Zambroni de Souza
Eliane Valença Nascimento de Lorenci

https://doi.org/10.22533/at.ed.5602119105

CAPÍTULO 6 72

ESTUDOS DE TRANSITÓRIOS ELETROMAGNÉTICOS E ELETROMECÂNICOS" DA ENERGIZAÇÃO DA LT 500KV AYOLAS-VILLA HAYES SEM REATOR DESDE A CENTRAL HIDRELÉTRICA ITAIPÚ

Elisandro Rodriguez Buzarquis
Rodney Damián Fariña Martínez
Antônio Carlos Zambroni de Souza

https://doi.org/10.22533/at.ed.5602119106

CAPÍTULO 7 86

TRANSMISSÃO DE ENERGIA SEM FIO POR MEIO DE ACOPLAMENTO MAGNÉTICO RESSONANTE COM METAMATERIAIS CONVENCIONAIS E SUPERCONDUTORES

Arthur Henrique de Lima Ferreira
Lucas Douglas Ribeiro
Rose Mary de Souza Batalha

https://doi.org/10.22533/at.ed.5602119107

CAPÍTULO 8 96

DEGRADAÇÃO POR POTENCIAL INDUZIDO (PID): REVISÃO

Hellen Ferreira Barreto Miranda
Luan Peixoto da Costa
Stefhany Oliveira Soares
Jonathan Velasco da Silva

https://doi.org/10.22533/at.ed.5602119108

CAPÍTULO 9 108

CAPACITOR BANK ALLOCATION IN DISTRIBUTION SYSTEMS USING THE DISCRETE PSO ALGORITHM

Luís Henrique Chouay Dall' Agnese
Carlos Roberto Mendonça da Rocha

https://doi.org/10.22533/at.ed.5602119109

CAPÍTULO 10 119

DESIGN OF A TRANSMISSION-LINE METAMATERIAL WITH A NEGATIVE INDEX OF REFRACTION AT S-BAND

Lucas Douglas Ribeiro
Juscelino Júnior de Oliveira
Arthur Henrique de Lima Ferreira
Rose Mary de Souza Batalha

https://doi.org/10.22533/at.ed.56021191010

CAPÍTULO 11 129

RADIO PROPAGAÇÃO E MODELAGEM PARA UMA PONTE SOBRE O RIO TOCANTINS

PARA LTE
Alaim de Jesus Leão Costa
Thiago Eleuterio da Silva
Diego Kasuo Nakata da Silva
Leslye Estefania Castro Eras
https://doi.org/10.22533/at.ed.56021191011

CAPÍTULO 12..141

TESTES DE IMUNIDADE CONTRA SURTOS ELÉTRICOS EM ELETRODOMÉSTICOS
Gustavo Oliveira Cavalcanti
Marcílio André Félix Feitosa
Kayro Féllyx Henrique Pereira
Manoel Henrique da Nóbrega Marinho
Antonio Samuel Neto
Lucas de Carvalho Sobral
Pollyana Maria Ramos Gonçalves
Douglas Thiago Moreira Lara
Thiago Francisco Gomes
Renato Jardim Teixeira
Wagner Almeida Barbosa
https://doi.org/10.22533/at.ed.56021191012

CAPÍTULO 13..152

AUTOMAÇÃO DA ILUMINAÇÃO E EFICIÊNCIA ENERGÉTICA EM EDIFICAÇÕES - O SISTEMA DE CONTROLE DE ILUMINAÇÃO DALI: UM ESTUDO DE CASO
Marcos Noboru Kurata
Ênio Carlos Segatto
https://doi.org/10.22533/at.ed.56021191013

CAPÍTULO 14..163

INFLUÊNCIA DAS VARIÁVEIS AMBIENTAIS E CONSTRUTIVAS NO EIXO DO ROTOR EÓLICO
Leonardo Pavan
Evandro André Konopatzki
Cristiane Lionço de Oliveira
https://doi.org/10.22533/at.ed.56021191014

CAPÍTULO 15..172

VIABILIDADE DO SISTEMA FOTOVOLTAICO NA REGIÃO DO RECÔNCAVO DA BAHIA
Gabriel Garcia Bastos de Almeida
Luanna Valéria Sousa Fonseca
Andréa Jaqueira da Silva Borges
https://doi.org/10.22533/at.ed.56021191015

SOBRE OS ORGANIZADORES 183

ÍNDICE REMISSIVO...184

CAPÍTULO 2

OPTOELECTRONIC SENSOR APPLIED TO FLOW RATE MEASUREMENTS ON OIL AND GAS INDUSTRY

Data de aceite: 01/10/2021
Data de submissão: 06/07/2021

Alexandre Silva Allil
Electrical Engineering Program (PEE), Federal University of Rio de Janeiro (UFRJ)
Rio de Janeiro – RJ
https://orcid.org/0000-0002-2753-7014

Fabio da Silva Dutra
Research Center Leopoldo Amèérico Miguez de Mello (CENPES - Petrobras)
Rio de Janeiro – RJ
https://orcid.org/0000-0003-3612-8148

Cesar Cosenza de Carvalho
Electrical Engineering Program (PEE), Federal University of Rio de Janeiro (UFRJ)
Rio de Janeiro – RJ
https://orcid.org/0000-0002-5221-708X

Regina Célia da Silva Barros Allil
Electrical Engineering Program (PEE), Federal University of Rio de Janeiro (UFRJ)
Rio de Janeiro – RJ
https://orcid.org/0000-0001-5823-5927

Marcelo Martins Werneck
Electrical Engineering Program (PEE), Federal University of Rio de Janeiro (UFRJ)
Rio de Janeiro – RJ
https://orcid.org/0000-0002-8804-0503

ABSTRACT: A flare system in oil platform is a combustion stack used to burn off excess gases that cannot be processed and gases that have to be eliminated in emergency shutdown to avoid the risk of explosion. Gas flow measurement in flares is still considered challenging because the measurement has to attend many specific demands, quite different from any other flow measurement applications. For these types of measurements many sensor technologies are available, however they are all very expensive, and only a few ones can attend all demands. The objective of this letter is to present a flow rate sensor based on Fiber Bragg Grating (FBG), cross-correlation and heatwave travel time techniques. The system was developed with inexpensive components and is little-intrusive, capable of attaining the rangeability of the flare demand and independent of gas composition, pressure and temperature.
KEYWORDS: Cross-correlation, Fiber Bragg grating (FBG), Flare systems, Flow rate, Optical fiber sensor.

SENSOR OPTOELETRÔNICO APLICADO A MEDIDAS DE VAZÃO NA INDÚSTRIA DE ÓLEO E GÁS

RESUMO: Um sistema de alívio (*Flare*) na plataforma de petróleo é uma chaminé de combustão usada para queimar gases em excesso que não podem ser processados e gases que devem ser eliminados em desligamentos de emergência para evitar o risco de explosão. A medição do fluxo de gás em *flares* ainda é considerada um desafio porque a medição deve atender a muitas demandas específicas, totalmente diferente de qualquer outra aplicação de medição de fluxo. Para esses tipos de medição, muitas tecnologias de sensores estão

disponíveis, porém todas são muito caras e apenas algumas podem atender a todas as demandas. O objetivo deste trabalho é apresentar um sensor de vazão baseado em Redes de Bragg (*FBG*), técnicas de correlação-cruzada e tempo de viagem por ondas de calor. O sistema foi desenvolvido com componentes de baixo custo e pouco intrusivo, capaz de atingir a rangeabilidade da demanda do *flare* e independe da composição do gás, pressão e temperatura.
PALAVRAS-CHAVE: Correlação-cruzada, Rede de fibra de Bragg (*FBG*), Sistemas de alívio, Vazão, Sensor à Fibra Óptica.

1 I INTRODUCTION

The oil and gas industry is responsible for a significant share of the greenhouse gas emissions. In the exploration and production of natural gas and oil, the gas which is burned in torches, known as flare or relief system, is a huge source of CO_2 emissions.

A typical flare system is a combustion stack used to burn off excess gases that cannot be processed. It is also used as a safety measure in emergency shutdown when gases in the process plant have to be eliminated to avoid the risk of explosion.

In addition to contributing to global warming and climate change, the burning of natural gas is considered a waste of valuable, nonrenewable energy resource.

In this context, the need to quantify the waste of gas volumes correctly and accurate is evident. Due to the importance of this fact, frequent publications of regulatory directives are issued, aiming at improving the measurements of gas flow in flare systems.

Nowadays, the gas flow measurement in flares is performed with very expensive equipment and it is still considered challenging because the measurement is quite different from other flow measurement applications.

The following challenges are still to be overcome when measuring flow in flares (Shannon, 2017):

- Unpredictable nature of gas flaring, since the petroleum gas is a varied mixture of gaseous hydrocarbons whose main component is always methane CH_4.
- Velocity range and accuracy. During 98% of total operating time the range may vary from a meager 0.03 m/s up to 5 m/s, which is the normal plant operation (known as pilot or purge). Accuracy demands are around 10%;
- Gas temperature may vary from -70°C to above 150°C;
- Size of flare systems. The burner line diameter may vary from 8'' to 40'';
- Being the flare an important safety equipment, flowmeters should not impinge any impedance in the flow so that conventional flowmeters based on turbine, orifice plate, Coriolis and Vortex cannot be applied on flares.

Several technologies are available for flow velocity measurement. The most used technologies are:

- Ultrasonic Flow Meter. It measures the difference in transit time of pulses that travel from a downstream transducer to the upstream transducer and vice versa. It is highly accurate but presents a high cost per installation, ranging from $50,000 - $100,000 (Sage Metering, 2020);
- Pitot Tube. This is the oldest way to measure flow velocity, it is based in a differential pressure to determine the flow velocity. It presents low flow sensitivity and its response depends on the gas composition;
- Thermal mass flow meter. Their working principle is based on the measurement of the heat convection from a heated surface to the flowing fluid as the sensor temperature is proportional to the mass flow rate. This the most commonly method to measure the mass flow of clean and unmixed gases or gases mixtures when the gas composition is consistent and known. Since this technique is based on the thermal properties of the fluid it is dependent upon fluid composition (Steinberg, 2013);
- Optical flow meters. They are divided into two classes, Laser Doppler velocimeters (LDV) and Doppler-Laser-Two-Focus Velocimetry (L2F). LDV is based in the Doppler shift of a laser beam to measure the velocity where two beams of laser cross the flow being measured generating fringes. L2F method, also known as Laser Transit Anemometry, measures the time of flight (ToF) of particles crossing the two laser beams (Ruck, 1994). These two optical methods are independent of pressure, temperature and gas composition but are based on the presence of sub-micrometer size particles in the gas that shall be inserted by the system (Parker, 2007).

In conclusion from the challenges and technologies listed above, all flowmeters present good performance in some aspects but bad performance in others. Normally, the choice goes to the most expensive one, the ultrasonic flowmeter.

Another important feature that is preferable in equipment applied to the oil and gas industry is the capability of working without embarked electricity. This is because electrically passive equipment does not depend on the expensive security technology for protection against fire and explosions. In this sense, fiber optic sensors tend to be cheaper and less complex to install and maintain.

The objective of this paper is to present a flow rate sensor based on Fiber Bragg Grating (FBG), cross-correlation and heatwave travel time techniques. The system is inexpensive and minimum intrusive, capable of attaining the rangeability of the flare demand and independent of gas composition, pressure and temperature.

2 | CROSS-CORRELATION TECHNIQUE

The cross-correlation (CC) is frequently applied when one needs to recognize a short-duration signal inserted in a longer signal. CC presents many applications, such as in pattern recognition, for instance in biometric recognition of retina or fingerprint, or tracking a person through a camcorder through face recognition (Wu, 2010). Other application of CC is presented in the work of (Wenbiao, 2009), who studied cross-correlation for application in velocimetry using electrostatic sensors. The result of the CC algorithm is a measurement of similarity between two signals against the displacement of one of them along the time. CC is used in signal processing and is defined as the correlation of a series against another series, shifted by a particular number of samples.

The CC algorithm is easily understood when we exam the algorithm applied to produce it.

Suppose two time series ($\mathcal{X}_{\mathcal{K}}$, $\mathcal{Y}_{\mathcal{K}}$) having $\mathcal{M}$ samples each by Equations (1) and (2).

$$[x_k] = [x_0, x_1, x_2, \dots, x_{M-1}] \quad (1)$$

$$[y_k] = [y_0, y_1, y_2, \dots, y_{M-1}] \quad (2)$$

Then, the cross-correlation function, $\phi_{yx}(\tau)$, is defined as Equation (3).

$$\phi_{yx}(\tau) = \sum_{t=0}^{M-1} x_\tau y_{t+\tau} \quad (3)$$

Where τ is the time delay.

3 I FIBER BRAGG GRATING

Fiber Bragg grating is a modulation of the refractive index of the core of an optical fibers, forming a grating. This grating reflects a narrow band of the light guided in the fiber, centred at the Bragg wavelength, according to the Bragg law (Werneck, 2017) of Equation (4).

$$\lambda_B = 2\eta_{eff}\Lambda \quad (4)$$

Where λ_B is the Bragg wavelength, η_{eff} is the effective refractive index of the core and Λ is the periodicity of the grating. Essentially, any external agent capable of changing Λ or η_{eff} will displace the reflected spectrum centered at $\lambda_{\mathcal{B}}$, either a longitudinal deformation or a temperature variation. The sensitivity of the Bragg wavelength with temperature is given by Equation (5).

$$\frac{\Delta\lambda_B}{\lambda_B} = (\alpha_{FBG} + \eta)\Delta T \quad (5)$$

Where $\Delta\lambda_B$ is the Bragg wavelength shift, ΔT is the temperature variation, α_{FBG} is the silica thermal expansion coefficient $\alpha_{FBG} = 0.55 \times 10^{-6}/ \,^{o}C$ and η is thermo-optic coefficient for a Ge-doped silica optical fiber $\eta = 8.6 \times 10^{-6} / ^{o}C$. Thus, the sensitivity of the grating to temperature at the wavelength range of 1550 nm is $\Delta\lambda_B/\Delta T = 14.18\ pm / ^{o}C$.

4 I MATERIALS AND METHODOLOGIES

The general idea of the proposed system it to apply a current signal on a heat source upstream inside the duct. The heat source is initially comprised by a small resistor, which will be changed in the future by a laser source injecting light into an optical fiber with its tip coated with an absorbing material to generate heat. In this work we tested only the resistor as a heat source; the methods to produce the heat with laser are under study. As a result of the heat pulse, a sub-degree temperature variation will flow inside the duct at the same speed as the gas. When this temperature pulse reaches the sensors, they will respond accordingly with a time delay. But due to the fact that the heat produced will be vanishing along the tube, the two sensors will detect different signal intensities. In order to detect the time delay, a CC algorithm is employed and the flow velocity is calculated by the ratio between the sensors distance and the time delay.

This technique was mentioned by the first time by (Xu, 1996) that used thermistors to measure flow velocity. They tested at flow speeds up to 30 mm/s, clearly far below from what is needed for flare flow measurement.

It is good to notice that (Ashauer, 1993) demonstrated a ToF technique using thermocouples, but the measured velocities were in the range of millimeters per second, not obtaining a linear relationship for flow velocities above 16 mm/s.

Additionally, (Fernandes, 2010) applied the ToF and CC techniques to measure newborn air breathing velocity using two lasers beams perpendicular to the respiratory flow and two position sensor detectors (PSDs) as sensors. They demonstrated a good linearity in the flow velocity measurement up to 1 m/s.

The schematic diagram of the proposed system in this paper is shown in Figure 1, where *d* is the distance between the two temperature sensors, FBG_1 and FBG_2.

The CC detects the few-milliseconds delay between the two pulses and the flow velocity can be calculated by the ratio between the sensors distance *d* and the time delay τ.

The airflow is obtained by a turbine that controls the airflow velocity in a wind tunnel (see Figure 1), by the motor speed and a Pitot tube is used for calibration.

The FBG interrogator is a Micron Optics model si155 with 5 kHz interrogation frequency and ±2 pm resolution.

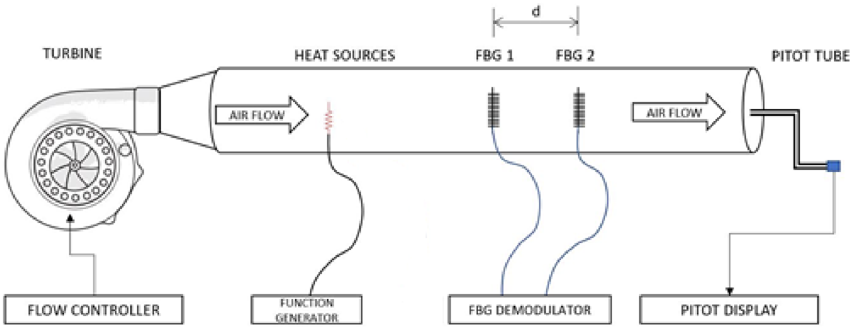

Figure 1 - Schematic diagram of the system inside the wind tunnel.

The Figure 2 shows a picture of the experimental setup, the wind tunnel and the sensors.

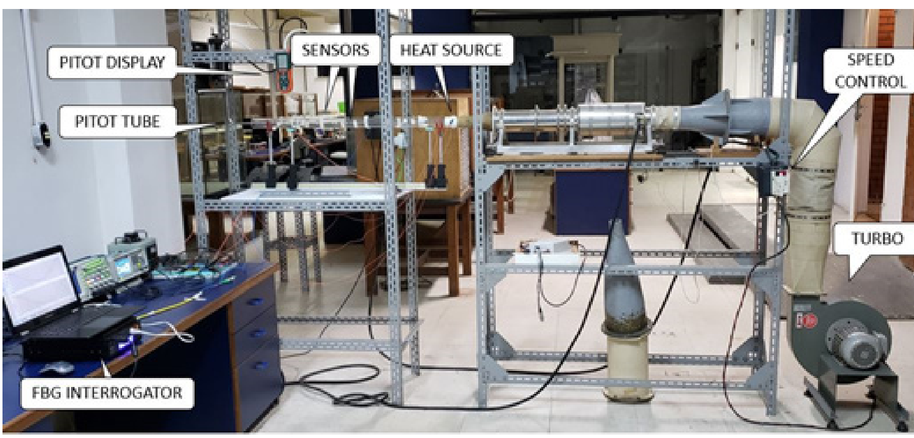

Figure 2 - Picture of the wind tunnel and the sensors location.

5 I RESULTS AND DISCUSSION

The Figure 3 shows the signals collected from the FBGs for a flow rate of 5 m/s. The blue line represents the output from the proximal FBG, while the orange line represents the output from the distal FBG. The signal-to-noise ratio is low because the temperature pulses collected by the FBGs are too close to the accuracy of the interrogation equipment, ±2 pm, recalling that 1°C in an FBG represents about 14 pm displacement of its central wavelength.

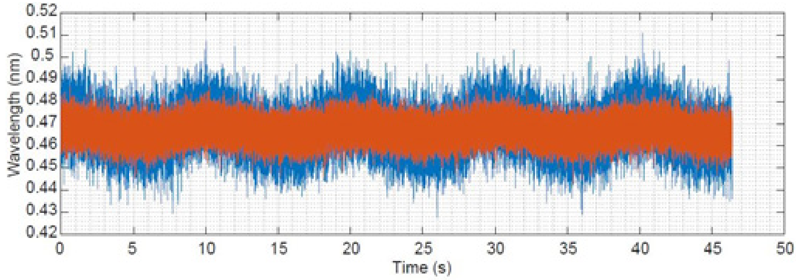

Figure 3 - The output signals produced by the two FBGs at a flow rate of 5 m/s. The signal-to-noise ratio is too small to allow any temperature variation distinction. Blue line: FBG_1;
Orange line: FBG_2.

As expected, no direct cross-correlation is possible with this low signal-to-noise ratio, as the noise produced by the interrogation equipment modifies differently each signal, making them absolutely uncorrelated. In order to clear the signals from the noise, a low-pass, first-order Butterworth filter was applied using Matlab software. The command used is [*b*,*a*] = *butter* (n,W_n) which returns the transfer function coefficients of an n^{th} order lowpass digital Butterworth filter with normalized cutoff frequency W_n.

The command returns *b* and *a* which are row vectors of length *n+1*, representing the coefficients of the filter's transfer function. We decided by a second-order filter ($n = 2$) and the cut-off frequency to be W_n = 850 mHz because the heat pulse frequency was 500 mHz. Since n = 2, vectors *a* and *b* will contain 3 numbers each, that are used on the transfer function of the digital filter, at Equation (6).

$$H(z) = \frac{B(z)}{A(z)} = \frac{b(1) + b(2)z^{-1} + b(3)z^{-2}}{a(1) + a(2)z^{-1} + a(3)z^{-2}} \quad (6)$$

However, since filters change signal phase and since the signals shown in Figure 3 are different from each other, even using the same filter one can change differently the phase in each signal, disturbing the cross-correlation results. In order to circumvent this effect, the MatLab function *filtfilt* was used. The syntax is *y* = *filtfilt* (*b*,*a*,*x*) that performs a zero-phase digital filtering by processing the input data, *x*, which contains 125,000 points, in both forward and reverse directions.

The result of this operation is a zero-phase distortion with a transfer function equals to the squared magnitude of the original filter and an order that is double the order specified by *b* and *a*.

The Figure 4 shows the result of these two operations applied in real time to the signals shown in Figure 3.

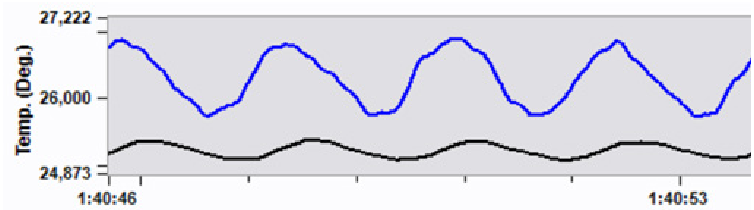

Figure 4 - Temperature signals captured by the two FBGs as a result of the signal processing techniques applied to the signals shown in Figure 3. The upper line (blue) represents the temperature sensed by FBG1 and the bottom line (black) the temperature sensed by FBG2. Horizontal axis shows time (h:m:s).

Notice that the delay between the signals is now visible and that, while the proximal sensor measured a pulse of about 1°C, the distal sensor measured only about 0.2°C. This temperature, according to the FBG sensitivity to temperature shown above, represents a Bragg wavelength shift of only 5 pm, too close to ±2 pm, the FBG interrogator accuracy.

Before applying the CC procedure, it is necessary to perform another signal processing, because the two signals shown in Figure 3, although with a noticeable phase delay, are completely different from each other, both in shape and in amplitude. Any attempt to cross-correlate these signals would result in a triangular-shape output with zero delay, meaning no correlation at all. To circumvent this, we have to normalize both signals by the average and the standard deviation using the Matlab command: *T* = (*a*-*mean*(*a*))/*std*(*a*) where *a* stands for each series.

Finally, Figure 5 shows the result of the CC algorithm performed in Matlab on the signals shown in Figure 4 after normalization. The maximum probability occurred at a delay of 135 ms.

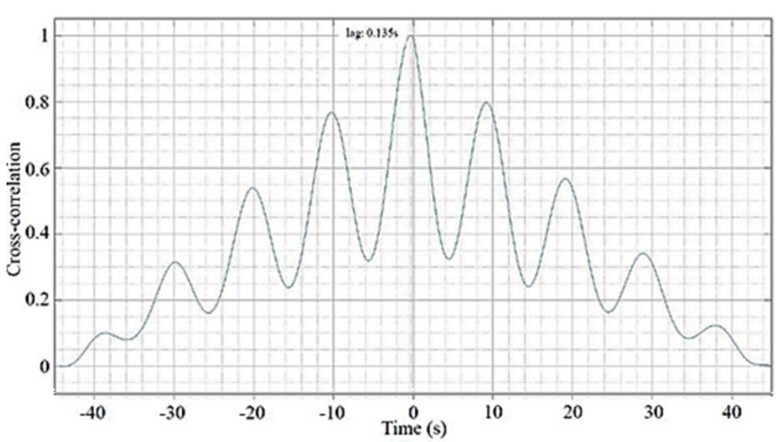

Figure 5 - The cross-correlation results. Y-axis plots the probability of similarity whereas X-axis plots the time delay.

From this calculated delay, corresponding to the lag time that the heat pulse takes to travel 77 cm from the upstream sensor to the downstream sensor, it is possible to calculate an airflow velocity of approximately 5.70 m/s.

This process was repeated twenty times each, for different velocities resulting in the plot shown in Figure 6.

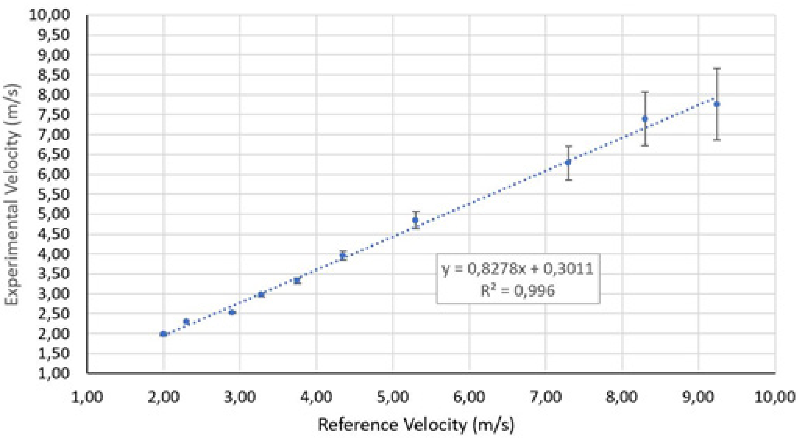

Figura 6 - Plot of the measured velocity by the FBG system versus calibrated velocity measured by the Pitot tube.

Notice that, while for flow velocities up to 6 m/s the standard deviations are smaller than 5%, for higher velocities, the error bars increase substantially reaching up to 10% for speeds higher than 9 m/s. The reason for this is attributed to two limitations: The first one is the sampling rate provided by the commercial interrogator. It produces output values at regular frequency, rather from being continuous, which causes phase errors in the CC calculations. The second reason is its ±2 pm Bragg wavelength uncertainty, leading to limitations in detecting sub-degree-centigrade temperatures.

High-precision ToF measurement is the main request to flow rate measurement of ultrasonic gas flowmeters and also for the system presented in this work. However, the measurement accuracy of CC depends on high-speed of an analogical-to-digital converter (ADC), which is not the case of commercial interrogators.

In order to improve the accuracy and resolution of ToF measurements, (Sun, 2019) proposed the cross-correlation calculation performed after digital filtering and interpolation. Such technique worked well in our case but only up to 10 m/s. For higher speeds the conclusion is that, either the sampling rate needs to be implemented or an interrogation system with continuous output signal be applied.

To circumvent these limitations, we propose the use of a bench-top interrogation technique such as those employed in (Dante, 2019) consisting of wavelength-division multiplexing (DWDM) or Fabry-Perot edge filters, respectively, which provide a higher output sensitivity to FBG center wavelength displacement, together with a continuous, real-time output.

6 I CONCLUSIONS

A new methodology to measure volumetric flow rate inside flare ducts based in heatwave travel time, FBG and cross-correlation techniques was presented. Results demonstrate that the system attend the main demands for a flare flowmeter showing independence of gas composition, good linearity and accuracy and low cost as compared to conventional flowmeters. On the top of that, the system can be built so as to not require electricity for its operation, promising to be a good candidate for an all-fiber explosion-proof system.

The system presented a linear behavior for flow velocities measurement up to a velocity of 10 m/s. Flow velocities above that present an up to 10% precision, due to limitations of the commercial interrogation system used.

It is suggested an edge filter interrogation technique to be applied in future tests to interrogate the FBGs in order to improve signal-noise-ratio, allowing the measurement of higher velocities.

ACKNOWLEDGMENTS

The authors acknowledge the valuable support from Petrobras whose guidance and assistance are gratefully acknowledged.

REFERENCES

Dante, A; Lopez, J.; Allil, R.; Carvalho, C.; Werneck, M.; **A Compact FBG-based Magnetostrictive Optical Current Sensor with Reduced Mass of Terfenol-D**, IEEE Photonics Technology Letters, page(s): 1-4 DOI: 10.1109/LPT.2019.2932112. July, 2019.

Fernandes, C.W.; M.D. Bellar and M.M. Werneck, **Cross-Correlation Based Optical Flowmeter. IEEE Transactions on Instrumen-tation & Measurement**, Volume 59 Issue 4, pp 840 - 846, DOI 10.1109/TIM.2009.2025990, March, 2010.

J. Wu, H. Yue, Y. Cao and Z. Cui, **Video Object Tracking Method Based on Normalized Cross-correlation Matching**, Ninth International Symposium on Distributed Computing and Applications to Busi-ness, Engineering and Science, Hong Kong, 2010, pp. 523-527. doi: 10.1109/DCABES.2010.112.

M. Ashauer, H. Glosch, F. Hedrich, N. Hey, H. Sandmaier, W. Lang, **Thermal flow sensor for liquids and gases based on combinations of two principles**. Sensors and Actuators 73 1999. 713.

Parker, J.; Stobie, G.; Melnyk, I., Letton, C.; **Flare Metering with Optics from Blue-Sky Technology to the Real World**. 25th International North Sea Flow Measurement Workshop, Oslo, Norway, October 16-19, 2007.

Ruck, B., Pavlovski, B., Semidetnov, N., **Phase-two-focus anemometer for simultaneous measurement of particle velocity and particle size**. Flow Measurement and Instrumentation, Volume 5, Issue 3, July 1994, Pages 195-202.

S. Sun, S. Li, L. Lin, Y. Yuan and M. Li, **A Novel Signal Processing Method Based on Cross-correlation and Interpolation for ToF Measurement**, 2019 IEEE 4th International Conference on Signal and Image Processing (ICSIP), Wuxi, China, 2019, pp. 664-668. doi: 10.1109/SIPROCESS.2019.8868700.

Sage Metering, Inc. [Online]. **3 Flare Gas Flow Meter Technologies**. Available at: https://sagemetering.com/flare-gas-meter/flare-gas-flow-meter-technologies/. Accessed on: July, 28, 2019.

Shannon, W., **The Challenges and Solutions of Flare Gas Metering. A Sage Metering**, [Online]. Available at: https://sagemetering.com/wp-content/uploads/2017/08/Challenges-Solutions-Flare-Gas-Measurement.compressed.pdf. Accessed on: July, 28th, 2019.

Steinberg, B, **Flare Gas Measurement Using Thermal Mass Flow Meters**, A Sage Metering White Paper, 2013. Available: https://sagemetering.com/pdf-doc/articles-whitepapers/Flare-Gas-Measurement-UsingThermal-Mass-Flow-Meters-0713.pdf.

Wenbiao Zhang, Chao Wang, Liang Li, Tao Zhang, Yong Yan, Jiaqing Shao, Wuliang Yin, **Parameters Selection in the Cross-Correlation Based Velocimetry Using Electrostatic Sensors**. I2MTC 2009 - International Instrumentation and Measurement Technology Conference, Singapore, 5-7 May 2009.

Werneck, M.M.; Regina C. Allil and Fbio V. de Nazar, **Fiber Bragg Gratings: Theory, Fabrication, and Applications** - Tutorial Texts in Optical Engineering, Volume TT114, 256 pages, SPIE PRESS, Bellingham, Washington USA, ISBN 9781510613850q (softcover), Date Published: 5 September 2017.

Xu, Y; G. de Graaf and R. F. Wolffenbuttel, **DSP Cross-Correlator for Use in a Thermal Flow Meter**. IEEE Instrumentation and Measurement Technology Conference, Brussels, Belgium, pp. 519-522, June 4-6, 1996.

ÍNDICE REMISSIVO

A

Acoplamento magnético ressonante forte 84

Automação de iluminação 150

C

Cálculo de perdas de energia 39

Composto direito/esquerdo (CRLH) 117

Controle da iluminação 150

Correlação-cruzada 15

Custos anuais de construção de linhas de distribuição 39

D

Detecção 94, 154

Durabilidade de rede de Bragg 25

E

Eficiência energética 7, 150, 151, 153, 160

Encapsulamento 25, 27, 29, 30, 31, 32, 35

Energia eólica 161, 162, 168

Enlace analógico a fibra óptica 1, 13

Enlace fotônico sob baixa polarização 1

Estruturas periódicas 117

F

FBG 5, 14, 15, 16, 18, 19, 21, 22, 23, 25, 26, 27, 28, 29, 30, 32, 35, 36, 37

Fotovoltaico 7, 94, 170, 172, 173, 174, 175, 176, 177, 178, 179, 180

Fuzzy Logic 5, 54, 55, 65, 68

I

Índice de refração negativo 117

Inteligência artificial 55

L

Lei de Kelvin 38, 39

LTE 7, 118, 125, 127, 128, 129, 136, 137

M

Metamateriais 6, 84, 117

N

Neuro-Fuzzy 127, 129, 130, 133, 134, 136, 137

O

Otimização estática 39

P

Perda de propagação 127, 128, 136

Permeabilidade negativa 117

Permissividade negativa 117

PID 6, 94, 95, 96, 97, 98, 99, 100, 101, 102, 103, 104, 105

Planejamento de potência reativa 106

Proteção contra surtos 139, 140

R

Rádio propagação sobre pontes 127

Rede de fibra de Bragg (FBG) 15

Refrigerador 139, 140, 141, 146, 147, 148

Reversão 94

Revisão literária 94

RFBG 5, 25, 26, 27, 28, 31, 32

RF em fotônica 1

Rotação 161, 162, 164, 166, 167, 168, 169

S

Sensor à fibra óptica 15

Sistema DALI 150, 154, 155

Sistemas de alívio 15

Sistemas de distribuição 106, 115, 141

Sistemas de potência 106

Supercondutividade 84

Surtos elétricos 7, 139, 140, 141, 142, 144, 146, 148, 149

T

Televisor 139, 140, 141, 144, 145

Transmissão de energia sem fio 6, 84

V

Vazão 14, 15

Velocidade do vento 161, 163, 164, 165, 166, 167, 168

Vida útil 47, 139, 140, 141, 147, 148, 170

COLEÇÃO

DESAFIOS DAS ENGENHARIAS:

ENGENHARIA ELÉTRICA 2

www.atenaeditora.com.br

contato@atenaeditora.com.br

@atenaeditora

www.facebook.com/atenaeditora.com.br

Atena Editora

Ano 2021

COLEÇÃO

DESAFIOS DAS ENGENHARIAS:

ENGENHARIA ELÉTRICA 2

www.atenaeditora.com.br

contato@atenaeditora.com.br

@atenaeditora

www.facebook.com/atenaeditora.com.br

Atena Editora

Ano 2021